

Fiber-Reinforced Alkali-Activated Materials Based on Waste Materials [†]

Martin Mildner ^{*}, Jan Fořt  and Robert Černý 

Department of Materials Engineering and Chemistry, Faculty of Civil Engineering, Czech Technical University in Prague, Thákurova 7/2077, 166 29 Prague, Czech Republic

^{*} Correspondence: martin.mildner@fsv.cvut.cz

[†] Presented at the 10th MATBUD'2023 Scientific-Technical Conference "Building Materials Engineering and Innovative Sustainable Materials", Cracow, Poland, 19–21 April 2023.

Abstract: The adverse effects associated with a rise in global temperature require substantial advances in various industries, the building industry in particular, with an emphasis on sustainability and circular economy measures. Research effort on the design of alkali-activated materials with sufficient engineering properties is thus on the rise, as these materials form a possible way to replace cementitious binders in the future. This paper deals with the description of an alternative material without the use of cementitious binders. The alkaline activation of a blended precursor composed of a finely ground granulated blast furnace slag and metashale, activated using waste alkalis from industrial production is studied. In addition, this material was reinforced using 25 mm long fibers of a waste fiberglass reinforcement fabric to improve the mechanical properties. This research confirmed the suitability of using a range of waste or secondary raw materials to produce new materials which then have lower environmental impacts.

Keywords: alkali activation; metashale; blast furnace slag; waste alkali activator; waste fibers

1. Introduction

Cement composites have become irreplaceable elements in the construction industry over the last few decades due to their properties and low production costs. However, their production involves the consumption of significant quantities of raw materials and primary energy for manufacturing. Moreover, the production and transport of cement place a high CO₂ burden on the environment [1,2]. Despite all drawbacks, cement is the most widely used building material in the world due to its superior engineering properties. In terms of their environmental impact and material properties, alkali-activated materials (AAM) seem to be a suitable option and they also match the development direction of building materials due to the valorization of various by-products or industrial waste products [3].

AAMs are formed by the alkaline activation of aluminosilicates (precursors) using highly alkaline activators. The precursors are usually obtained as waste materials or secondary raw materials from industrial production (blast furnace slag, silica fume, metashale and metakaolin), but natural precursors (rice husk, palm oil ash) can be used as well. Through the utilization of various waste or natural precursors, the production of binders and the associated release of CO₂ are noticeably reduced. As activators, water glass or hydroxide are the most commonly used [4–6]. Apart from being aggressive substances, their production, which is very energy-demanding, also represents a substantial burden on the natural environment and human health. For this reason, waste alkalis, which can also be obtained as waste raw materials from industrial production, should be used instead [7]. The selection and use of the precursors and activators significantly influence the final properties of the AAM, such as the mechanical, thermal or electrical properties, as well as their fire and frost resistance [8,9]. In regards to the properties of AAM, some of them can



Citation: Mildner, M.; Fořt, J.; Černý, R. Fiber-Reinforced Alkali-Activated Materials Based on Waste Materials. *Mater. Proc.* **2023**, *13*, 1. <https://doi.org/10.3390/materproc2023013001>

Academic Editors: Katarzyna Mróz, Tomasz Tracz, Tomasz Zdeb and Izabela Hager

Published: 13 February 2023



Copyright: © 2023 by the authors. Licensee MDPI, Basel, Switzerland. This article is an open access article distributed under the terms and conditions of the Creative Commons Attribution (CC BY) license (<https://creativecommons.org/licenses/by/4.0/>).

also be modified by adding fiber reinforcement to the material's matrix. The use of fibers can also lead to a reduction in the cracks arising from debonding, sliding and pull-out [10].

Glass fibers are synthetic amorphous silicates that are commonly available at low cost. Their main advantage is their high flexural strength [11]. Pernica et al. [12] studied a Na geopolymer E-glass composite and observed an increase in the flexural strength from 175.9 to 255.2 MPa. Sankar and Kriven [11] observed the behavior of geopolymer-reinforced E-glass lazy weaves and observed an increase in the flexural tensile strength as well.

This study aimed to assess the potential of waste or secondary raw materials as the main sources for the production of new alternative building materials. In addition to the waste precursor, the alkaline activator represents a waste material from industrial cleaning operations and can also be viewed as waste material. In other words, this research contemplated the production of alternative AAMs based on waste materials, with a significantly reduced environmental footprint. Thus, the utilization of selected waste products can be seen as beneficial in terms of the environment and cost savings achieved by avoiding costly disposal. To improve the mechanical properties and reduce the shrinkage of the material, waste glass fibers were utilized.

2. Experiments

2.1. Materials

The precursor used to produce the alkali-activated material was a combination of two aluminosilicates materials: finely ground granulated blast furnace slag (produced by Kotouč Štramberk, Czech Republic) and metashale (produced by České Lupkové Závody, A.S., Czech Republic). Finely ground granulated blast furnace slag (GGBFS) is a secondary raw material from iron production. Metashale (RON D460 HR) is produced by heat treatment of the waste material from metashale Mefisto L05 production. Both precursors are shown in Figure 1 and their chemical composition is presented in Table 1.



Figure 1. (a) Finely ground granulated blast furnace slag (GGBFS); (b) metashale (RON D460 HR).

Table 1. Chemical composition of the precursors used.

| Precursor | SiO ₂ | Al ₂ O ₃ | Fe ₂ O ₃ | TiO ₂ | MgO | CaO | K ₂ O | MnO | SO ₃ | LOI |
|-------------|------------------|--------------------------------|--------------------------------|------------------|-----|------|------------------|-----|-----------------|-----|
| GGBFS | 39.1 | 9.8 | 0.5 | 0.3 | 8.7 | 38.8 | 0.7 | 0.9 | 0.6 | 0.6 |
| RON D460 HR | 49.1 | 47.3 | 0.9 | 1.6 | 0.1 | 0.2 | 0.5 | — | — | 0.3 |

Waste alkalis (WAA) based on sodium hydroxide from the industrial processes of glass production (AGS Glass, Teplice, Czech Republic) were used as an alkaline activator. These alkalis are in solid form in the form of pellets (see Figure 2), from which an activating solution of the appropriate molarity is produced. For the purpose of this research, an 8 M solution of WAA was used.



Figure 2. (a) Solidified waste alkalis based on sodium hydroxide (WAA); (b) fibers from the waste fiberglass reinforcement fabric (WFF).

Fibers from waste fiberglass reinforcement fabric (WFF) were used to reinforce the alkali-activated composite. This fabric is very important for ensuring high quality and a strong final layer in the interior plaster. The fabric was cut into individual fibers 25 mm in length (see Figure 2). The producer reported that the minimal tensile strength of the fiber is from 2000 to 2200 N/50 mm, while the elongation is 3.5%.

A mixture of fine standard aggregate in three fractions (0.08–0.5, 0.5–1.0 and 1.0–2.0 mm) was used for the mortar samples.

The experimental program was divided into two sets of sample mixtures. One set of samples was without WFF; the other had WFF fibers. The procedure for mixing the WFF was as follows. The mixture was mixed one step at a time. First, the dry components (a mixture of the respective precursors and fine aggregates) were mixed and then an 8 M solution of WAA was added. At the very end, WFF fibers were inserted in batches to avoid the fibers clumping in the matrix.

The individual mixtures differed in the percentage of the respective precursors, i.e., GGBFS and RON, which changed after 20%. The composition of the studied mixtures is shown in Table 2.

Table 2. Composition of 1 m³ of the studied mixtures.

| Mixture Designation | GGBFS (kg) | RON (kg) | Fibers WFF (kg) | Fine Aggregate (kg) of Fractions | | | Solution of 8 M WAA (kg) |
|---------------------------------------|------------|----------|-----------------|----------------------------------|------------|------------|--------------------------|
| | | | | 0.08–0.5 mm | 0.5–1.0 mm | 1.0–2.0 mm | |
| (a) Composition with fibers | | | | | | | |
| 80S+20R | 460 | 115 | | | | | |
| 60S+40R | 345 | 230 | | | | | |
| 40S+60R | 230 | 345 | 5.1 | 380 | 380 | 380 | 296 |
| 20S+80R | 115 | 460 | | | | | |
| (b) Composition without fibers | | | | | | | |
| 80S+20R | 460 | 115 | | | | | |
| 60S+40R | 345 | 230 | | | | | |
| 40S+60R | 230 | 345 | — | 382 | 382 | 382 | 297 |
| 20S+80R | 115 | 460 | | | | | |

2.2. Experimental Methods

2.2.1. Chemical and Mineralogical Properties

The phase composition of the measured mixtures was studied by X-ray diffraction (XRD). Diffractograms were recorded using a Malvern PANalytical Aeris diffractometer equipped with a CoK α source operating at 7.5 mA and 40 kV. The incident beam's path consisted of iron beta-filter, Soller slits at 0.04 rad and a divergence slit at 1/2°.

For measurement by XRF analysis, a sequential WD-XRF spectrometer (ARL 9400 XP, Thermo ARL) was used, which was equipped with a Rh anode tipped X-ray tube (type 4 GN) fitted with a 50 μ m Be window.

2.2.2. Basic Material Properties

The bulk density and matrix density of each mixture in the hardened state were determined. Bulk density was determined on dried samples by measuring them with a digital caliper and then weighing them. The matrix density was determined using a helium pycnometer (Pycnomatic ATC, Thermo Scientific, Waltham, MA, USA). The open porosity of the samples was calculated from these values.

2.2.3. Mechanical Properties

Flexural and compressive tensile strengths were tested after 28 days of curing under laboratory conditions (20 °C and 50% RH). Three prismatic specimens of 40 × 40 × 160 mm from each mix were tested each time for flexural tensile strength and then for compressive strength on the resulting fractures. An ED60 hydraulic press was used for the measurements.

2.2.4. Analyzing the Microstructure of the Surface

Scanning electron microscopy (SEM) was used to document where the matrix material interfaced with the blended fibers. A test sample measuring 40 × 40 × 160 mm was cut using a saw into 1 mm slices, which were then used for SEM. A Phenom XL (ThermoScientific) was used with a magnification range of 80 to 100,000×.

3. Results and Discussion

3.1. Basic Material Properties

The basic characteristics of the material such as the bulk density, matrix density and the open porosity of the material calculated from them are shown in Table 3. There was no clear trend in the open porosity values of the different mixtures. The results were more or less similar for all measured mixtures and oscillated around the average value. The mixture labeled 80S+20R is slightly out of line, having the highest measured value of 19.82%. This is probably due to measurement uncertainty.

Table 3. Basic material properties of the mixtures.

| Mixture Designation | Bulk Density (kg/m ³) | Matrix Density (kg/m ³) | Open Porosity (%) |
|---------------------|-----------------------------------|-------------------------------------|-------------------|
| 80S+20R | 2025 | 2525 | 19.82 |
| 60S+40R | 2022 | 2495 | 18.97 |
| 40S+60R | 2039 | 2500 | 18.44 |
| 20S+80R | 2026 | 2506 | 19.18 |

3.2. Chemical and Mineralogical Properties

Alkaline activation increased the amorphous matter content and also caused the formation of a zeolitic structure, diffracting at low angles. As the slag content increased, the amount of amorphous matter increased as well (see Figure 3). It may be observed that the phase composition of alkali-activated S+R mixtures (Table 4) reflects the gradually changing composition of the mixed precursors.

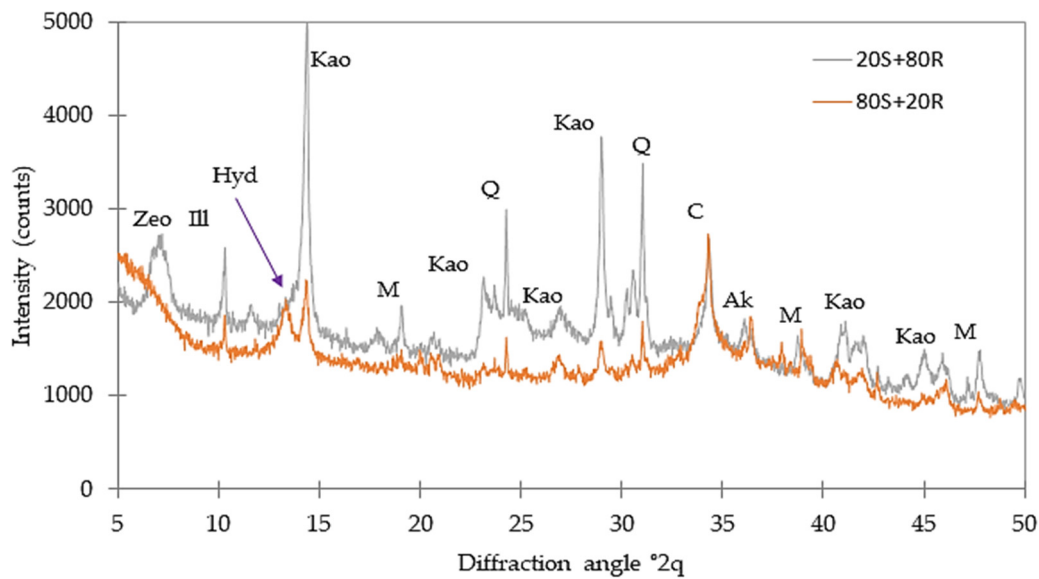


Figure 3. Comparison of two extreme activated products: 20S+80R and 80S+20R. Explanatory notes: Kao, kaolinite; Ill, illite; Zeo, zeolitic structure; Hyd, hydrotalcite; Ak, akermanite; C, calcite; Q, quartz; M, mullite.

Table 4. Phase composition of the mixtures (XRD analysis).

| Minerals | Formula | Individual Phase Content (%) | | | |
|-----------------|---|------------------------------|---------|---------|---------|
| | | 80S+20R | 60S+40R | 40S+60R | 20S+80R |
| Amorphous phase | — | 80 | 75 | 63 | 61 |
| Calcite | CaCO ₃ | 3 | 4 | 5 | 4 |
| Quartz | SiO ₂ | 0 | 0 | 2 | 3 |
| Akermanite | Ca ₂ Mg(Si ₂ O ₇) | 5 | 4 | 3 | 2 |
| Merwinite | Ca ₃ Mg(SiO ₄) ₂ | 3 | 2 | 2 | 0 |
| Kaolinite | Al ₂ (OH) ₄ Si ₂ O ₅ | 2 | 6 | 11 | 13 |
| Illite | K _{0.65} Al _{2.0} [Al _{0.65} Si _{3.35} O ₁₀](OH) ₂ | 2 | 5 | 6 | 6 |
| Mullite | Al ₆ Si ₂ O ₁₃ | 1 | 3 | 5 | 8 |
| Zeolite | — | 0 | 0 | 0 | 1 |
| Hydrotalcite | Mg ₆ Al ₂ CO ₃ (OH) ₁₆ ·4H ₂ O | 4 | 4 | 2 | 2 |

The amount of R-related phases (kaolinite, illite, mullite) decreased, while the amount of slag-related minerals (akermanite, merwinite) increased with the slag content. Interestingly, the calcite content was about the same in all samples. This might indicate that akermanite also undergoes some kind of alteration in an alkaline environment. The zeolite-like structure was clearly apparent only in the 20S+80R; the lower R content caused its merge in low-angle intensity to increase. Hydrotalcite was observed as clear crystalline product of activation; its content increased with the slag dosage (magnesium and carbonate anions both come from slag).

3.3. Mechanical Properties

The mortar specimens (the samples were 40 × 40 × 160 mm in dimension) were tested for basic mechanical properties, i.e., flexural tensile strength and compressive strength. The mechanical properties were investigated both on specimens produced without the addition of WFF and on separate specimens with WFF added. Both strengths (flexural and compressive tensile) were tested over a standard period of 28 days.

Figure 4 below shows the results of the individual flexural tensile strength tests. As expected, the specimens without waste fibers showed lower values for these strengths. The

highest values were achieved by the 60S+40R blend in both cases (without and with WFF). The flexural tensile strength of the samples with WFF fibers was 8.96 MPa, an improvement of nearly 27% in these strengths.

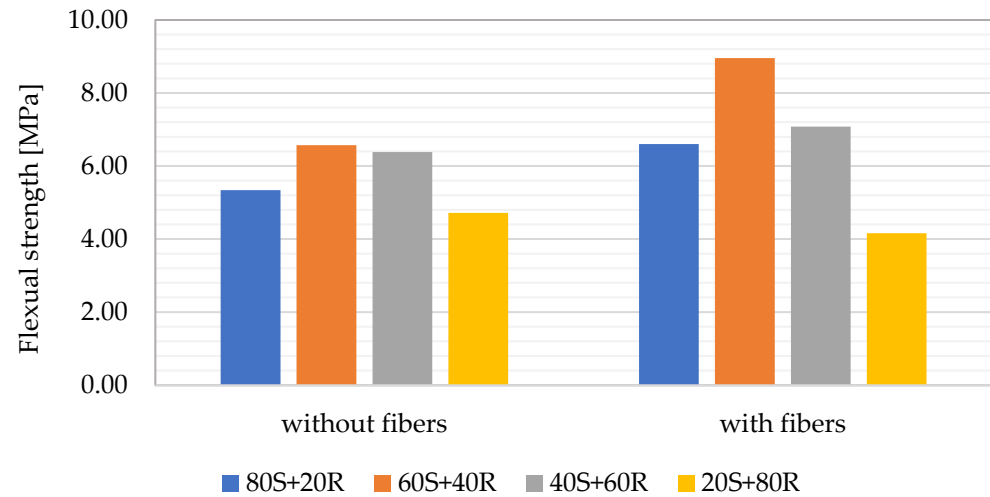


Figure 4. Comparison of the flexural strength of samples without and with WFF fibers.

For the mixture labeled 20S+80R, the final strengths deteriorated and decreased after the addition of fibers. This phenomenon was caused by the poor precursor ratio. A large amount of RON D460 HR metashale did not produce good strengths under alkaline activation.

The compressive strength (Figure 5) of the specimens was tested on fractions of the specimens after the flexural tensile strength test. Again, the compressive strength of the fiber specimens without WFF was highest for the mixture marked 60S+40R, which achieved 46.9 MPa. There was a slight increase in the compressive strength after the addition of WFF fibers. For the 60S+40R blend, the increase was below 10 MPa.

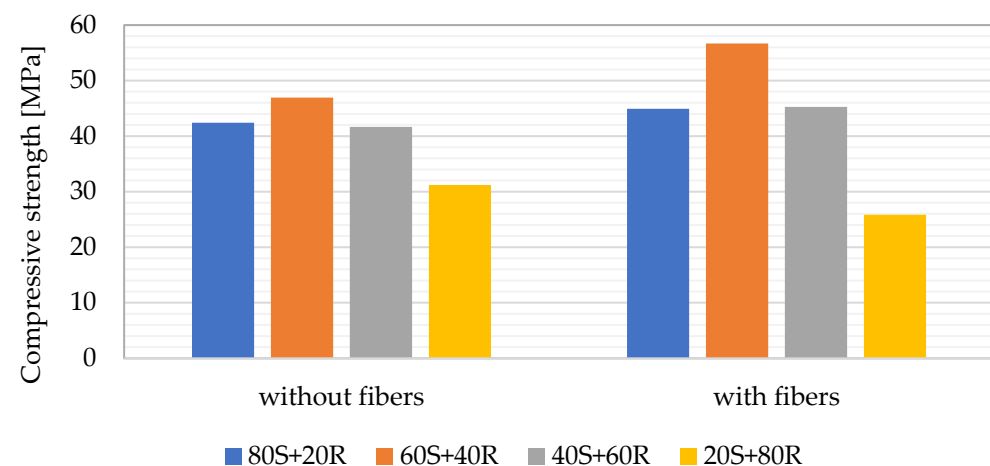


Figure 5. Comparison of the compressive strength of samples without and with WFF fibers.

The best blend in terms of mechanical properties appeared to be a blend of the alkali-activated composite with 60% GGFBS and 40% RON D460 HR within the precursor blend. The fibers helped to improve the structure and thus increased the flexural and compressive tensile strengths of the alkali-activated material.

3.4. Scanning Electron Microscopy (SEM)

Scanning electron microscopy (SEM) was used to investigate the surface of the alkali-activated composite. The aim was to capture the interface between the WFF fibers and

the sample matrix, and to map any surface changes or micro-cracks in the material (see Figure 6).

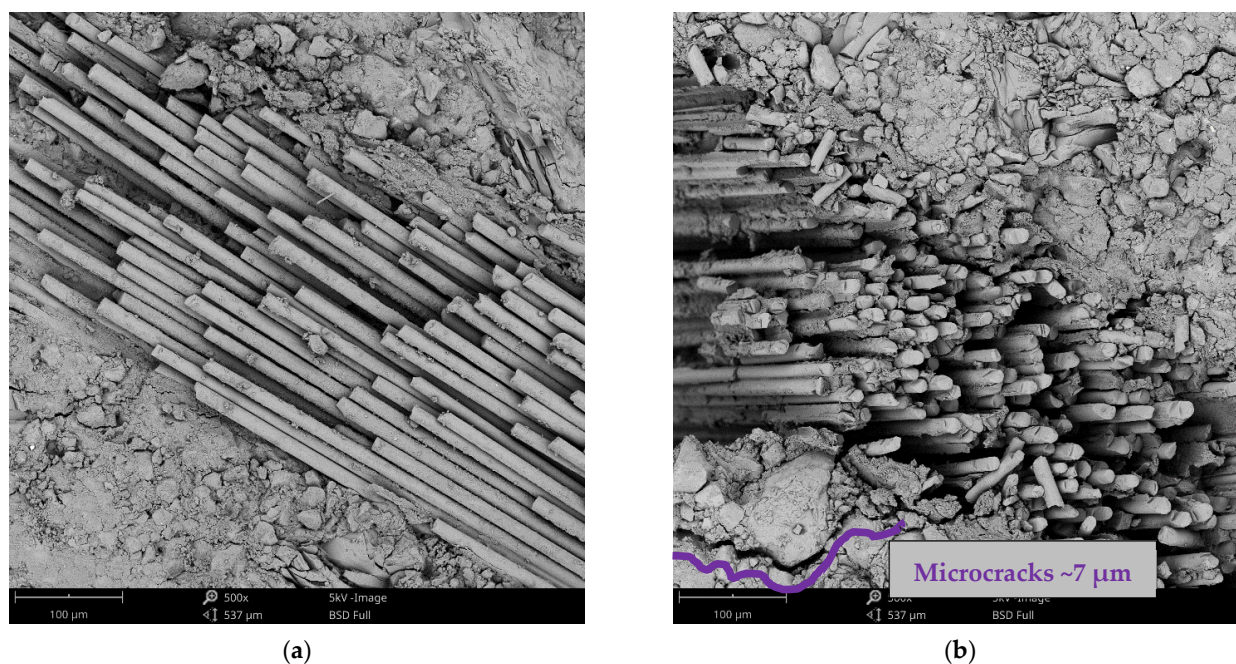


Figure 6. (a) The interface between the fiber and the matrix. (b) Structure of the material with microcrack-trapping fibers.

In Figure 6a, a single strand of the fibers can be seen, in which the individual glass fibers can be seen due to the cut. The quality of the interconnection between the fibers and the sample matrix can be seen. This resulted in a stronger and more durable material structure. In Figure 6b, the ability of the fibers to prevent the propagation of microcracks (shown in purple in the figure) is more evident. The size of the microcracks in the samples was around 7 μm. The largest microcrack captured was 20 μm.

4. Conclusions

This study considered the utilization of various waste materials in the form of upcycling to design environmentally friendly reinforced materials that may be viewed as an alternative to cementitious materials. For this purpose, a blended precursor composed of waste metashale and ground granulated blast furnace slag was activated by a waste cleaning solution and reinforced by waste fiberglass. The results obtained indicated the successful integration of the WFF into the material's matrix without any distinct segregation or the formation of microcracks on the interface. Increasing the metashale from 20% to 40% resulted in a positive effect on the mechanical properties, specifically from 42 MPa to 47 MPa in compressive strength without fibers and from 45 MPa to 57 MPa with fibers. However, a further increase in the metashale content reduced both the flexural and compressive strength. The most beneficial effect of applying fibers was seen for the combination of 60% slag and 40% metashale. In general, the mechanical strength of the designed materials reached a sufficient level and can be deemed to be a viable way for future follow-up work aiming to precisely determine the optimal ratio of the components.

Author Contributions: Conceptualization, J.F. and R.Č.; methodology, J.F. and R.Č.; software, M.M.; validation, J.F. and R.Č.; formal analysis, J.F. and R.Č.; investigation, J.F. and M.M.; resources, J.F.; data curation, M.M.; writing—original draft preparation, M.M. and J.F.; writing—review and editing, J.F.; visualization, M.M.; supervision, J.F.; project administration, R.Č.; funding acquisition, R.Č. All authors have read and agreed to the published version of the manuscript.

Funding: This research was funded by the support of M.era-Net Call 2021, Project No. 9262 and financial support from Technology Agency of Czech Republic under project TH80020002 and by the Czech Technical University in Prague under project No. SGS22/137/OHK1/3T/11.

Institutional Review Board Statement: Not applicable.

Informed Consent Statement: Not applicable.

Data Availability Statement: Not applicable.

Acknowledgments: The publication cost of this paper was covered by funds from the Polish National Agency for Academic Exchange (NAWA): “MATBUD 2023—Developing international scientific cooperation in the field of building materials engineering” BPI/WTP/2021/1/00002, MATBUD 2023.

Conflicts of Interest: The authors declare no conflict of interest.

References

1. Zhang, H.; Kodur, V.; Cao, L.; Qi, S. Fiber Reinforced Geopolymers for Fire Resistance Applications. *Procedia Eng.* **2014**, *71*, 153–158. [[CrossRef](#)]
2. Refaat, M.; Mohsen, A.; Nasr, E.A.R.; Kohail, M. Minimizing energy consumption to produce safe one-part alkali-activated materials. *J. Clean. Prod.* **2021**, *323*, 129137. [[CrossRef](#)]
3. Korniejenko, K.; Łach, M. Geopolymers reinforced by short and long fibers—Innovative materials for additive manufacturing. *Curr. Opin. Chem. Eng.* **2020**, *28*, 167–172. [[CrossRef](#)]
4. Parathi, S.; Nagarajan, P.; Pallikkara, S.A. Ecofriendly geopolymer concrete: A comprehensive review. *Clean Technol. Environ. Policy* **2021**, *23*, 1701–1713. [[CrossRef](#)]
5. Davidovits, J. Geopolymers and geopolymer new materials. *J. Therm. Anal.* **1989**, *35*, 429–444. [[CrossRef](#)]
6. Davidovits, J. *Geopolymer Chemistry and Applications*, 5th ed.; Institut Géopolymère: Saint-Quentin, France, 2020.
7. Fořt, J.; Mildner, M.; Keppert, M.; Černý, R. Waste solidified alkalis as activators of aluminosilicate precursors: Functional and environmental evaluation. *J. Build. Eng.* **2022**, *54*, 104598. [[CrossRef](#)]
8. Silva, G.; Kim, S.; Bertolotti, B.; Nakamatsu, J.; Aguilar, R. Optimization of a reinforced geopolymer composite using natural fibers and construction wastes. *Constr. Build. Mater.* **2020**, *258*, 119697. [[CrossRef](#)]
9. Liew, Y.M.; Kamarudin, H.; Al Bakri, A.M.; Luqman, M.; Nizar, I.K.; Ruzaidi, C.M.; Heah, C.Y. Processing and characterization of calcined kaolin cement powder. *Constr. Build. Mater.* **2012**, *30*, 794–802. [[CrossRef](#)]
10. Ranjbar, N.; Mehrali, M.; Mehrali, M.; Alengaram, U.J.; Zamin, M. Cement and Concrete Research Graphene nanoplatelet-fly ash based geopolymer composites. *Cem. Concr. Res.* **2015**, *76*, 222–231. [[CrossRef](#)]
11. Sankar, K.; Kriven, W.M. Geopolymer reinforced with E-glass leno weaves. *J. Am. Chem. Soc.* **2017**, *100*, 2492–2501. [[CrossRef](#)]
12. Pernica, D.; Reis, P.N.B.; Ferreira, J.A.M.; Louda, P. Effect of test conditions on the bending strength of a geopolymer-reinforced composite. *J. Mater. Sci.* **2010**, *45*, 744–749. [[CrossRef](#)]

Disclaimer/Publisher’s Note: The statements, opinions and data contained in all publications are solely those of the individual author(s) and contributor(s) and not of MDPI and/or the editor(s). MDPI and/or the editor(s) disclaim responsibility for any injury to people or property resulting from any ideas, methods, instructions or products referred to in the content.